Bioorganic & Medicinal Chemistry 18 (2010) 1227–1235

Contents lists available at ScienceDirect

Bioorganic & Medicinal Chemistry

journal homepage: www.elsevier.com/locate/bmc

Square pyramidal copper(II) complexes with forth generation fluoroquinolone and neutral bidentate ligand: Structure, antibacterial, SOD mimic and DNA-interaction studies

Mohan N. Patel *, Pradhuman A. Parmar, Deepen S. Gandhi

Department of Chemistry, Sardar Patel University, Vallabh Vidyanagar 388 120, Gujarat, India

ARTICLE INFO

Article history:
Received 25 September 2009
Revised 10 December 2009
Accepted 11 December 2009
Available online 22 December 2009

Keywords:
Gatifloxacin
Antimicrobial
pUC19
Superoxide anion
IC_{50}

ABSTRACT

Coordination of neutral bidentate ligand to copper ion in combination with gatifloxacin have been focused in this article. The effect of complexation reflects antibacterial activity, DNA interaction and SOD mimic activity of individual greatly. The geometry at the central metal ion provides a site for binding of superoxide anion responsible for better SOD mimic behaviour.

1. Introduction

Drugs are typically poly functional compounds, designed to interact with specific receptors or organs. Quinolone family drugs are frequently used to treat various bacterial infections because of their broad spectrum antibacterial activity.[1] Gatifloxacin [(±)-1-cyclopropyl-6-fluoro-1,4-dihydro-8-methoxy-7-(3-methyl-1-piperazinyl)-4-oxo-3-quinoline carboxylic acid] (GFLH) is fourth generation fluoroquinolone family antibacterial agent. It is a novel extended spectrum fluoroquinolone with an improved gram-positive and anaerobe coverage compared to older agents such as ciprofloxacin. GFLH acts intravenously by inhibiting topoisomerase II (DNA gyrase) or topoisomerase IV.[2] It is prescribed for treatment of acute bacterial exacerbation of chronic bronchitis, acute sinusitis, community acquired pneumonia, complicated and uncomplicated urinary tract infections (cystitis).[3]

It is evident that a variety of functional groups originate reactivity toward unforeseen targets such as metal cations. The design of metal–drug complexes are of particular interest in the pharmacological research. Metal combinations with pharmaceutical agents are known to improve the drugs activity, to decrease their toxicity and gain an ability to act as regulator for gene expression and a tool for microbiology.[4,5] Quinolone antibiotics are chelating agents for a variety of metal ions well known for their biological activity.[6–10] Probably the most widely studied cation in this respect is Cu(II) and is known to play a significant role either in naturally occurring biological systems or as pharmacological agents.[11] A low molecular weight copper complexes have been proven beneficial against several diseases such as tuberculosis, rheumatoid, gastric ulcers, and cancers.[12–15] Copper(II) complexes behave as an efficient chemical nuclease, when prepared by combination of drugs and nitrogen donor heterocyclic ligand, such as 2,2′-bipyridine and 1,10-phenanthroline, which act as NN donor ligands.[16,17] In a similar vein, the DNAase like activity of copper(II) with 1,10-phenanthroline have been widely documented.[18,19]

Nature provides a metalloenzyme named superoxide dismutases (SODs) to all living organism having oxygen as a part of metabolism which control the concentration of superoxide radical ($O_2^{\cdot-}$) tending to cause significant cellular damage by converting it to molecular oxygen and hydrogen peroxide and is implicated in many medical disorder.[20,21] A large number of mixed ligand copper(II) complexes have been known to exhibit superoxide dismutase like activity.[21–24] This activity depends on the Cu(II)/Cu(I) redox process, which is related to flexibility of the geometric transformation around the metal centre.[25] Herein we tends to develop a formulation of copper complexes using drug and some NN/NO donor ligands to get a complexes with better efficiency to act as DNA gyrase and for its enzymatic resemblance to SODs.

* Corresponding author. Tel.: +91 2692 226858x220.
E-mail address: jeenen@gmail.com (M.N. Patel).

0968-0896/$ - see front matter © 2009 Elsevier Ltd. All rights reserved.
doi:10.1016/j.bmc.2009.12.037

2. Result and discussion

2.1. Characterization of complexes

Several instrumental techniques like IR, UV–vis. spectroscopy, magnetic measurement and FAB-MS were used to evaluate structure of the complexes. Elemental analysis data are in good agreement with proposed structure. Table 1 comprises of physico-chemical parameters and Figure 1 represents the structure of the complex **1** (Supplementary 1: Structures of the complexes).

2.1.1. Spectrophotometric titration

The amount of copper is determine by spectrophotometric titration technique.[26,27] The calculated results from the equivalent endpoint (Fig. 2) reveals the metallic content of the complex (Table 2) (Supplementary 2: The spectrophotometric titration curves for equivalent endpoint determination of the complexes).

2.1.2. IR spectroscopy

In IR spectra of GFLH bands observed at 3437 cm^{-1}, 1611 cm^{-1}, 1332 cm^{-1} were attributed to the stretching vibration ν(H–O), $\nu(COO)_{asy}$, $\nu(COO)_{sym}$, respectively. On coordination with metal ion, the three bands of carboxylic group of GFLH have been replaced by two strong bands in the range 1563–1581 cm^{-1} [ν_{asym}(C=O)] and 1364–1377 cm^{-1} [ν_{sym}(C=O)]. The unidentate coordination mode of carboxylato ligand was characterized by $\Delta\nu$ value falling in the range 192–212 cm^{-1} [$\Delta\nu = \nu_{asym}(C{=}O) - \nu_{sym}(C{=}O)$].[28,29] Peak in range 1618–1627 cm^{-1} found in case of complexes were for pyridone oxygen ν(C=O) atom which appeared at 1718 cm^{-1} in gatifloxacin; this shift in band towards lower energy suggests coordination via pyridone oxygen atom.[30] These data were further supported by ν(M–O) which appear at ~513 cm^{-1}.[31] N→M bonding was supported by ν(M–N) band at ~545 cm^{-1}.[32] Some of the major IR bands are summarized in Table 3.

2.1.3. Electronic and magnetic behavior

Copper(II) complexes that is, d^9 system with a simple ligand at low temperature exhibit an absorption band with a large width make them very difficult to interpret. Complexes of copper(II) with different coordination numbers resulting in different geometry. The copper(II) complexes exhibit a broad band at ~15300 cm^{-1}[33–35] corresponding to a characteristic d–d transition in tetragonal field, suggesting distorted square pyramidal geometry for copper(II) complexes.

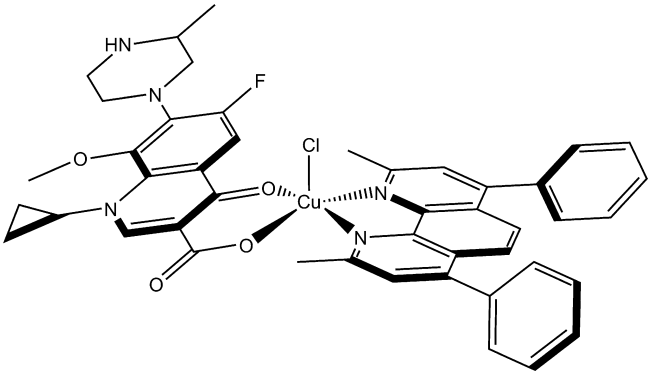

Figure 1. Structure of the title complex [Cu(L)(A1)Cl]·$5H_2O$.

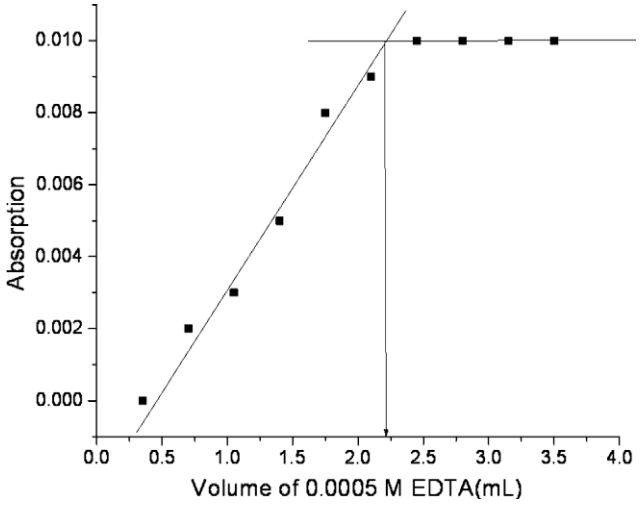

Figure 2. Experimental cure from the spectrophotometric determination of metal content of 9.96 mg complex [Cu(L)(A1)Cl]·$5H_2O$ dissolved in 20 ml of D.D. water by EDTA.

The magnetic moments measurement for any geometry in copper(II) complexes generally results in 1.8 BM, which is very close to spin-only value that is, 1.73 BM. The observed values in our case are very close to the spin-only values (Table 1) expected for $S = 1/2$ system (1.73 BM.) which lead to a path of conclusion that metal centre in synthesized complexes posses five coordination

Table 1
Physicochemical parameters and elemental details of the complexes

Empirical formula for complexes	Elemental analysis % required (found)				Mp (°C)	% Yield	$\mu_{eff.}$ BM	Formula weight (g/mol)
	C	H	N	Cu				
$C_{45}H_{51}ClCuFN_5O_9$ (**1**)	58.50 (58.51)	5.56 (5.57)	7.58 (7.56)	6.88 (6.87)	291	71.8	1.77	922.27
$C_{33}H_{43}ClCuFN_5O_9$ (**2**)	51.36 (51.35)	5.62 (5.61)	9.07 (9.08)	8.23 (8.24)	288	63.4	1.77	770.20
$C_{30}H_{37}ClCuFN_5O_{10}$ (**3**)	48.32 (48. 34)	5.00 (5.02)	9.39 (9.37)	8.52 (8.51)	277	66.9	1.77	744.15
$C_{31}H_{37}ClCuFN_5O_{11}$ (**4**)	48.13 (48.14)	4.82 (4.80)	9.05 (9.06)	8.21 (8.21)	>300	68.2	1.87	772.15
$C_{31}H_{38}ClCuFN_6O_{11}$ (**5**)	47.21 (47.23)	4.86 (4.85)	10.66 (10.67)	8.06 (8.05)	298	75.3	1.92	787.16
$C_{29}H_{40}ClCuFN_6O_9$ (**6**)	47.41 (47.40)	5.49 (5.50)	11.44 (11.45)	8.65 (8. 64)	293	67.7	1.74	733.18
$C_{24}H_{35}ClCuFN_3O_{10}S$ (**7**)	42.67 (42.68)	5.22 (5.24)	6.22 (6.21)	9.41 (9.40)	290	64.2	1.9	674.10
$C_{25}H_{36}ClCuFN_4O_{10}$ (**8**)	44.78 (44.77)	5.41 (5.40)	8.36 (8.38)	9.48 (9.46)	>300	61.5	1.85	669.14

Table 2
Spectrophotometric titration data for the complexes

Volume of 0.0005 M EDTA (mL)	Absorption at 745 nm							
	(**1**)	(**2**)	(**3**)	(**4**)	(**5**)	(**6**)	(**7**)	(**8**)
0.35	0	0.003	0	0	0.004	0	0	0.002
0.7	0.002	0.004	0.003	1.00E-03	0.005	0	0	0.002
1.05	0.003	0.006	0.004	0.003	0.006	0.002	0	0.004
1.4	0.005	0.007	0.005	0.005	0.007	0.004	0.003	0.004
1.75	0.008	0.007	0.006	0.006	0.008	0.005	0.005	0.006
2.1	0.009	0.009	0.008	0.008	0.009	0.007	0.007	0.007
2.45	0.01	0.01	0.009	0.01	0.009	0.008	0.01	0.007
2.8	0.01	0.011	0.01	0.011	0.01	0.009	0.012	0.008
3.15	0.01	0.011	0.01	0.011	0.01	0.01	0.013	0.009
3.5	0.01	0.011	0.01	0.011	0.01	0.01	0.013	0.009
Amount of complex dissolved in 20 ml (g)	0.00996	0.0102	0.01006	0.01018	0.00984	0.01028	0.01004	0.01032
Equivalents volume of 0.0005 M EDTA (mL)	2.160	2.654	2.677	2.609	2.491	2.839	2.947	3.034
Equivalent Concentration of EDTA at end point (M)	0.000108	0.000132	0.000134	0.000130	0.000125	0.000142	0.000147	0.000152
Amount of Cu in 2 mL (gm)	6.86297×10^{-5}	8.4351×10^{-5}	8.50563×10^{-5}	8.28958×10^{-5}	7.9236×10^{-5}	9.01972×10^{-5}	9.3645×10^{-5}	9.63853×10^{-5}
Amount of Cu in 20 mL (gm)	0.000686	0.000844	0.000851	0.000829	0.000792	0.000902	0.000936	0.000964
% Cu experimental	6.89	8.27	8.45	8.14	8.05	8.77	9.33	9.34
% Cu theoretically	6.88	8.23	8.52	8.21	8.06	8.65	9.41	9.48

Table 3
Characteristic absorptions bands of IR spectra of the complexes and GFLH (cm^{-1})

Compd	ν(C=O) pyridone	ν(H–O) carboxyl	$\nu(COO)_{asy}$	$\nu(COO)_{sym}$	$\Delta\nu$	ν(M–N)	ν(M–O)	ν(M–S)
GFLH	1718	3437	1611	1332	279	–	–	–
1	1620	–	1576	1375	201	540	520	–
2	1626	–	1581	1373	208	544	515	–
3	1627	–	1579	1361	212	533	519	–
4	1623	–	1568	1369	199	539	509	–
5	1619	–	1563	1365	198	541	510	–
6	1622	–	1577	1377	200	537	518	–
7	1624	–	1572	1374	198	–	512	431
8	1618	–	1580	1368	212	548	514	–

number with one unpaired electron responsible for $S = 1/2$ system.[36,37]

2.1.4. Thermogravimetric analysis

Thermogravimetric analysis was carried out using 5000/2960 SDTA, TA instrument (USA) operated at a heating rate of 10 °C per minute in the range of 20–800 °C under N_2 atmosphere. On interpretation of the thermogravimetric grams (Fig. 3: TG curve for complex **1**) three distinct weight losses were observed.[38] First weight loss occur between 50 to 120 °C, second between 180 to 430 °C and finally between 450 to 690 °C. Weight lost during first decomposition step corresponds to five molecules of crystalline

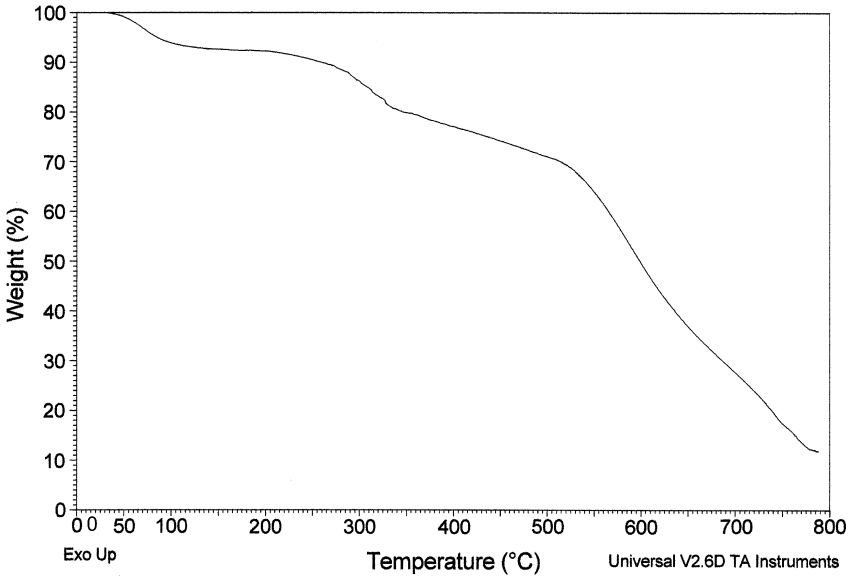

Figure 3. Thermal degradation curve of the complex **1** at heating rate of 10 °C per minute under N_2 atmosphere.

water, weight loss during second step corresponds to decomposition of neutral bidentate ligand where as third step corresponds to decomposition of GFL leaving behind CuO as a residue.

2.1.5. FAB-mass spectra

Figure 4 represents the FAB–mass spectrum of complex **1**, that is $[Cu(GFL)(A^1)Cl]\cdot 5H_2O$, obtained using *m*-nitro benzyl alcohol as matrix. Peaks at 136, 137, 154, 289 and 307 *m/z* value are due to usage of matrix. Peaks at 835 and 837 in spectra are assigned to (M) and (M+2) of complex molecule associated with three H^+ ion in absence of lattice water. There also exist a doublet at 764 and 766 for fragment of complex (*m/z* = 472) rid of neutral ligand associated with matrix (*m/z* = 289) and four H^+ ion. The doublet nature observed for case of two fragments suggests presence of one Cl atom. Several other fragments at 751, 576, 478, 309 and 203 *m/z* value are observed, attributed to fragments associated with matrix and H^+ ions, and fragments associated with H^+ ions alone. The proposed fragmentation pattern is shown in Supplementary data (Supplementary 3: Fragmentation pattern for complex 1).

2.2. Biological evaluation

2.2.1. In vitro antimicrobial screening

Table 4 shows in vitro antibacterial activity data of the synthesized complexes (**1**–**8**), ligands (A^1–A^8) and some fluoroquinolones, on a panel of bacterial strain such as *Escherichia coli* (*E. coli*), *Pseudomonas aeruginosa* (*P. aeruginosa*), *Staphylococcus aureus* (*S. aureus*), *Bacillus subtilis* (*B. Subtilis*), and *Serratia marcescens* (*S. marcescens*) as minimum inhibitory concentration (MIC, μM). From the data one can note down the following things:

(1) *S. aureus*: Complexes **1, 3, 4, 5** and **7** are much more active compare to all tested drugs and for said case complex **1** is the most potent one.
(2) *B. subtilis*: Complexes **1, 3, 4** and **5** are active compare to all, and complex **5** is prove to be most potent, whereas complexes 2, 6, 7 and **8** are active in comparison to enrofloxacin and gatifloxacin.
(3) *S. marcescens*: Except complexes 6 and **7** all are active than tested drugs where as complexes 1, 3 and **4** are found to be equipotent.
(4) *P. aeruginosa*: Complexes **1, 3, 4** and **5** are potent than tested drugs, out of which complex **4** is proved to be the most potent.
(5) *E. coil*: Complexes **1, 3, 4, 5** and **8** are potent compare to drugs tested here in, also the complex **5** is the most potent for the said case.

From the data comprise in Table 4 one can conclude that the complexes with phenanthroline and its derivatives are more active than other ligands like pyridine-2-carboxyaldehyde, 2,2′-bipyridylamine and thiophene-2-carboxyaldehyde. It can also be concluded that the almost all complexes possesses higher activity than GFLH and bidentate ligands. Thus this increase in antimicrobial activity may be studied under following five principles.[17,39–41]

I. The chelate effect, that is, ligands that are bound to metal ions in a bidentate fashion, such as the quinolones and phenanthroline, bipyridine or bipyridylamine show higher antimicrobial efficiency towards complexes with N-donor ligands.
II. Nature of the ligands.
III. The total charge of the complex; generally the antimicrobial efficiency decreases in the order cationic > neutral > anionic complex.
IV. The nature of the ion neutralizing the ionic complex.
V. The nuclearity of the metal center in the complex; dinuclear centers are usually more active than mononuclear ones.

Thus, first two factors may be consider for increase in the activity that is, chelation effect provided by drug and bidentate ligand.

2.2.2. DNA interaction study

2.2.2.1. Absorbance titration experiment. DNA can provide three distinct binding sites for quinolone metal complexes; namely, groove-binding, binding to phosphate group and intercalation.[42] This behavior is of great importance with regard to the relevant biological role of quinolone antibiotics in the body.[43,44] The absorption spectra of complexes **1**–**8** with DNA have been recorded for a constant complex concentration so as to have maximum absorbance up to unity with varying concentration of DNA so as to have different DNA:complex mixing ratios from 0 to 10.

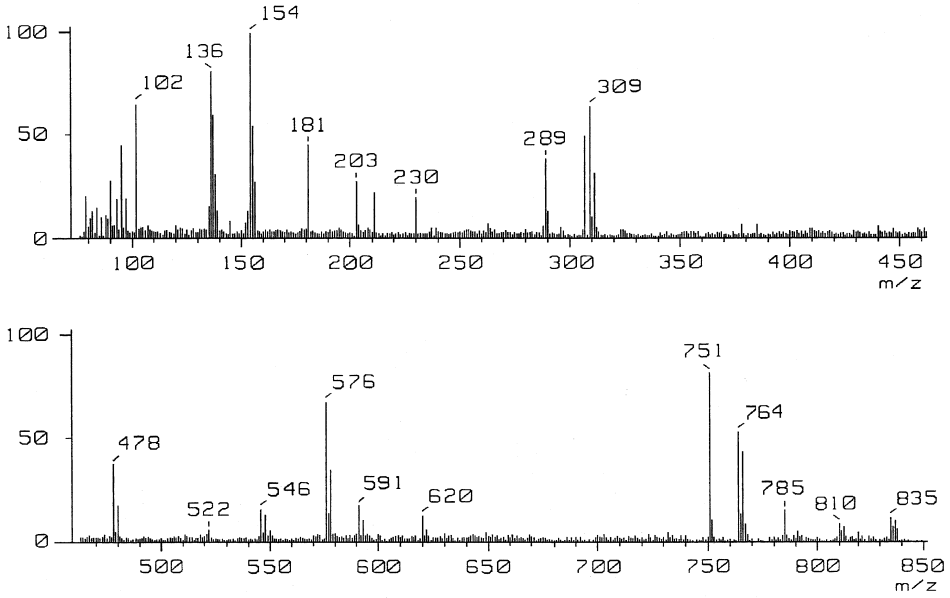

Figure 4. FAB-mass spectra of $[Cu(L)(A1)Cl]\cdot 5H_2O$ at the accelerating voltage was 10 kV.

Table 4
MIC in terms of μM

Compounds	Gram positive		Gram negative		
	S. aureus	*B. subtilis*	*S. marcescens*	*P. aeruginosa*	*E. coli*
$CuCl_2{\cdot}2H_2O$	2698.0	2815.0	2756.0	2404.0	3402.0
Ciprofloxacin	1.6	1.1	1.6	1.4	1.4
Gatifloxacin	5.1	4.0	2.9	1.0	2.9
Norfloxacin	2.5	2.5	4.1	3.8	2.8
Enrofloxacin	1.9	3.9	1.7	1.4	1.4
Pefloxacin	2.1	2.4	5.1	5.7	2.7
Levofloxacin	1.7	2.2	1.7	1.7	1.0
Sparfloxacin	1.3	2.0	1.5	1.5	1.3
Ofloxacin	1.9	1.4	1.7	2.2	1.4
A^1	194.0	169.0	272.0	255.0	278.0
A^2	130.0	250.0	506.0	154.0	129.0
A^3	631.0	670.0	604.0	725.0	758.0
A^4	829.0	733.0	771.0	738.0	762.0
A^5	578.0	631.0	609.0	658.0	591.0
A^6	3212.0	3271.0	3212.0	3183.0	3154.0
A^7	>10,000.0	>10,000.0	>10,000.0	>10,000.0	>10,000.0
A^8	3821.0	3414.0	3333.0	2902.0	3739.0
$[Cu(GFL)(A^1)Cl]{\cdot}5H_2O$ (**1**)	0.3	0.6	0.3	0.9	0.3
$[Cu(GFL)(A^2)Cl]{\cdot}5H_2O$ (**2**)	5.6	2.8	0.9	1.9	2.8
$[Cu(GFL)(A^3)Cl]{\cdot}5H_2O$ (**3**)	0.8	0.5	0.3	0.6	0.3
$[Cu(GFL)(A^4)Cl]{\cdot}5H_2O$ (**4**)	0.8	0.6	0.3	0.3	0.3
$[Cu(GFL)(A^5)Cl]{\cdot}5H_2O$ (**5**)	0.7	0.4	0.5	0.6	0.1
$[Cu(GFL)(A^6)Cl]{\cdot}5H_2O$ (**6**)	2.8	3.7	3.7	3.7	4.6
$[Cu(GFL)(A^7)Cl]{\cdot}5H_2O$ (**7**)	0.9	2.8	6.4	2.8	1.8
$[Cu(GFL)(A^8)Cl]{\cdot}5H_2O$ (**8**)	2.7	2.7	1.4	3.4	0.7

A representative spectrum is shown in Figure 5. The changes observed in the UV spectra of the complexes after mixing it with DNA (either the change in intensity or the shift of the wavelength) indicate that the interaction of complexes with DNA takes place by a direct formation of a new complex with double-helical DNA.[45] Extent of the binding strength of complexes was quantitatively determined by calculating intrinsic binding constants K_b of the complexes by monitoring the change in absorbance at various concentration of DNA. From the plot of $[DNA]/(\varepsilon_a-\varepsilon_f)$ versus [DNA], (Inset Fig. 5) the K_b value of complexes were determine and were found in the range 2.45×10^3–8.75×10^4 (Table 5). Which is much lower than the K_b value of classical intercalations (ethidium bromide) thus there is a possibility of intercalation in the complexes. Also, these values are closely comparable to some known complexes exhibiting covalent mode of binding,[46] which also suggests copper(II) ion prefers binding to guanine at N7 position.[47,48] Therefore, results indicate that complexes may first bind with phosphate group of DNA, neutralize the negative charge of DNA phosphate group, and cause the contraction and conformational change to DNA.

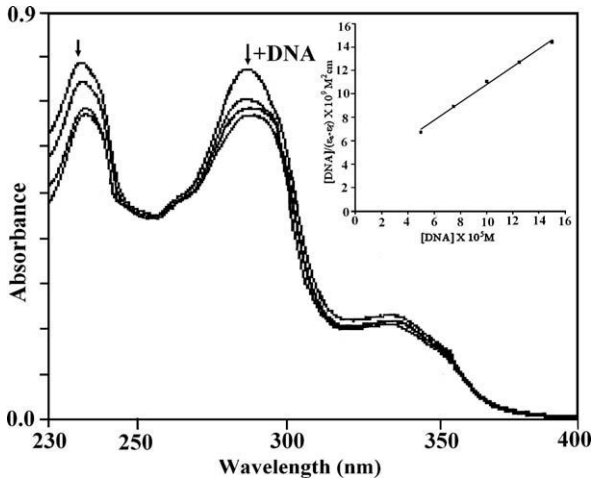

Figure 5. Electronic absorption spectra of $[Cu(L)(A1)Cl]{\cdot}5H_2O$ in phosphate buffer (Na_2HPO_4/NaH_2PO_4, pH 7.2) in the absence and presence of increasing amount of DNA. The [Cu] complex = 10 μM; [DNA] = 0–150 μM. The incubation period is 30 min at 37 °C, Inset: Plot of $[DNA]/(\varepsilon_a - \varepsilon_f)$ versus [DNA]. Arrow shows the absorbance change upon increasing DNA concentrations.

Table 5
The binding constants (K_b) of complexes with DNA in phosphate buffer pH 7.2

Complexes	K_b (M^{-1})
$[Cu(GFL)(A^1)Cl]{\cdot}5H_2O$ (**1**)	2.45×10^3
$[Cu(GFL)(A^2)Cl]{\cdot}5H_2O$ (**2**)	3.00×10^4
$[Cu(GFL)(A^3)Cl]{\cdot}5H_2O$ (**3**)	7.14×10^4
$[Cu(GFL)(A^4)Cl]{\cdot}5H_2O$ (**4**)	7.83×10^4
$[Cu(GFL)(A^5)Cl]{\cdot}5H_2O$ (**5**)	8.75×10^4
$[Cu(GFL)(A^6)Cl]{\cdot}5H_2O$ (**6**)	8.57×10^3
$[Cu(GFL)(A^7)Cl]{\cdot}5H_2O$ (**7**)	5.00×10^4
$[Cu(GFL)(A^8)Cl]{\cdot}5H_2O$ (**8**)	6.87×10^3

2.2.2.2. Viscosity titration. Interaction of DNA to complex by viscosity measurement in absence of crystallographic data and NMR data[49] can be regarded as a reliable tool. Intercalation of a molecule into DNA could result in lengthening, unwinding and stiffening of the helix and is usually accompany by increases in solution viscosity.[50–52] In our case increase in viscosity was observed hence complexes bind to DNA via intercalation mode and out of all, complex **5** interact more strongly compare to other (Fig. 6).

2.2.2.3. Gel electrophoresis; photo quantization techniques. Transition metal complex mediated DNA cleavage is the center of interest.[53,54] When plasmid DNA was subjected to electrophoresis after interaction, upon illumination of gel (Fig. 7) the fastest migration was observed for super coiled (SC) Form I, where as the slowest moving was open circular (OC) Form II and the intermediate moving is the linear (LC) Form III generated on cleavage of open circular. The data of plasmid cleavage are presented in Table 6. Here the complex **5** shows the maximum cleavage ability compare to all synthesized complexes. The different DNA-cleavage

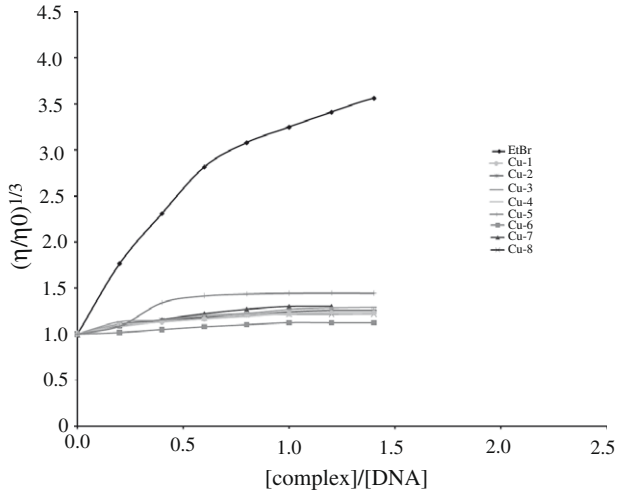

Figure 6. Effect on relative viscosity of DNA under the influence of increasing amount of complexes at 27 ± 0.1 °C in phosphate buffer (Na_2HPO_4/NaH_2PO_4, pH 7.2).

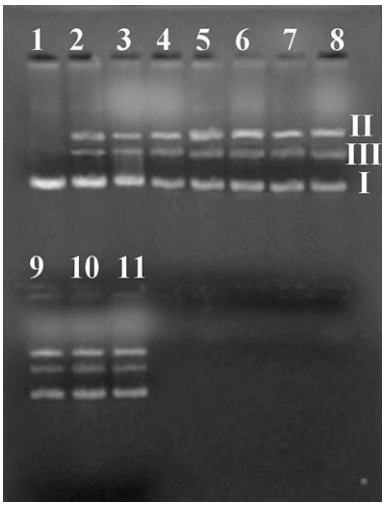

Figure 7. Photogenic view of cleavage of pUC19 DNA (300 μg/mL) with series of copper(II) complexes (200 μM) using 1% agarose gel containing 0.5 μg/mL ethidium bromide. All reactions were incubated in TE buffer (pH 8) in a final volume of 15 μL, for 24 h. at 37 °C. Lane 1, DNA control; Lane 2, $CuCl_2{\cdot}2H_2O$; Lane 3, Gatifloxacin; Lane 4, $[Cu(L)(A^6)Cl]{\cdot}5H_2O$; Lane 5, $[Cu(L)(A^7)Cl]{\cdot}5H_2O$; Lane 6, $[Cu(L)(A^8)Cl]{\cdot}5H_2O$; Lane 7, $[Cu(L)(A^2)Cl]{\cdot}5H_2O$; Lane 8, $[Cu(L)(A^1)Cl]{\cdot}5H_2O$; Lane 9, $[Cu(L)(A^3)Cl]{\cdot}5H_2O$; Lane 10, $[Cu(L)(A^4)Cl]{\cdot}5H_2O$; Lane 11, $[Cu(L)(A^5)Cl]{\cdot}5H_2O$.

Table 6
Complex mediated DNA cleavage data by gel electrophoresis

Lane No.	Compound	Form I	Form II	Form III
1	Control	100	—	—
2	$CuCl_2{\cdot}2H_2O$	66	24	10
3	Gatifloxacin	57	24	19
4	$[Cu(GFL)(A^6)Cl]{\cdot}5H_2O$ (**6**)	45	30	25
5	$[Cu(GFL)(A^7)Cl]{\cdot}5H_2O$ (**7**)	46	35	19
6	$[Cu(GFL)(A^8)Cl]{\cdot}5H_2O$ (**8**)	44	40	16
7	$[Cu(GFL)(A^2)Cl]{\cdot}5H_2O$ (**2**)	43	36	21
8	$[Cu(GFL)(A^1)Cl]{\cdot}5H_2O$ (**1**)	45	31	24
9	$[Cu(GFL)(A^3)Cl]{\cdot}5H_2O$ (**3**)	40	44	16
10	$[Cu(GFL)(A^4)Cl]{\cdot}5H_2O$ (**4**)	41	34	25
11	$[Cu(GFL)(A^5)Cl]{\cdot}5H_2O$ (**5**)	40	36	22

efficiency of the complexes, metal salt and drug is due to the difference in binding affinity of the complexes to DNA and the functionality present on ligand.

2.2.3. SOD-like activity: decomposition of reactive oxygen specie

NADH/PMS/NBT system was used to generate the superoxide radical artificially in order to check SOD like behavior of the complexes. The percentage inhibition of formazan formation at various concentrations of complexes as a function of time was determined by measuring the absorbance at 560 nm and plotted to have a straight line obeying equation $Y = mX + C$ (Fig. 8); with increase in concentration of tested complexes decrease in slope (m) was observed. Percentage inhibition of the reduction of nitro blue tetrazolium (NBT) plotted against the concentration of the complex (Fig. 9). Compounds exhibit SOD-like activity at biological pH with their IC_{50} values ranging from 0.5 to 1.775 μM (Table 7). The best IC_{50} value among synthesized complexes was observed for complex **5**. The higher IC_{50} can only be accredited to the vacant coordination site facilitating the binding of superoxide anion, electrons of aromatic ligands that stabilize $Cu{-}O_2^-$ interaction and not only to the partial dissociation of complex in solution. Plots for determination of IC_{50} values are placed in Supplementary data (Supplementary 4: Plots for determination of IC_{50} of complexes).

3. Conclusion

The complexes derived from phenanthroline derivatives are much more active compare to others. While comparing the data

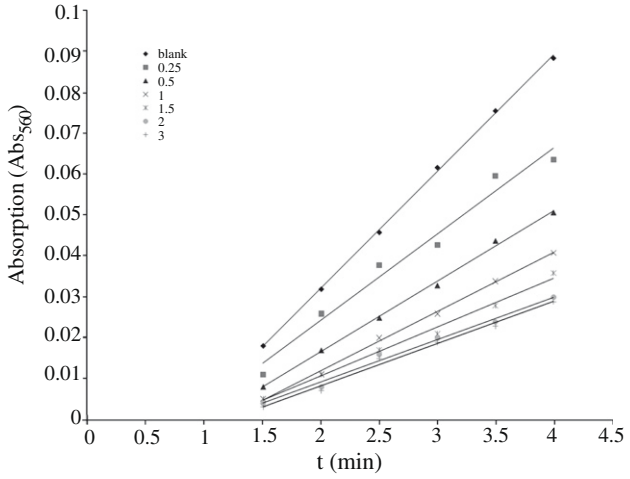

Figure 8. Absorbance values (Abs_{560}) as a function of time (t) plotted for varying concentration of complex **1** from 0.25 μM to 3 μM for which a good straight line are observed.

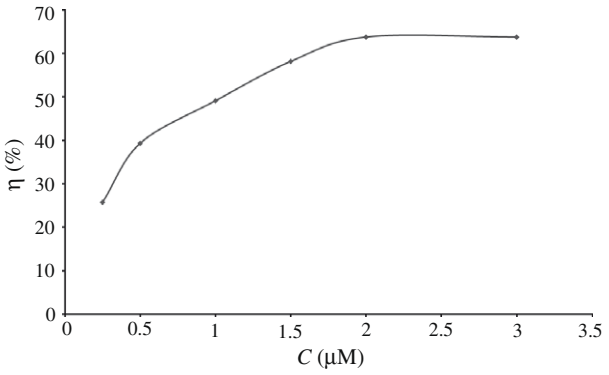

Figure 9. Plot of percentage of inhibiting NBT reduction with an increase in the concentration of complex **1**.

Table 7
Experimental values of IC_{50} obtain from non enzymatic SOD-like activities of synthesized complexes

Complexes	IC_{50} (μM)
$[Cu(GFL)(A^1)Cl]\cdot 5H_2O$ (**1**)	1.037
$[Cu(GFL)(A^2)Cl]\cdot 5H_2O$ (**2**)	0.775
$[Cu(GFL)(A^3)Cl]\cdot 5H_2O$ (**3**)	0.925
$[Cu(GFL)(A^4)Cl]\cdot 5H_2O$ (**4**)	0.875
$[Cu(GFL)(A^5)Cl]\cdot 5H_2O$ (**5**)	0.5
$[Cu(GFL)(A^6)Cl]\cdot 5H_2O$ (**6**)	1.125
$[Cu(GFL)(A^7)Cl]\cdot 5H_2O$ (**7**)	1.725
$[Cu(GFL)(A^8)Cl]\cdot 5H_2O$ (**8**)	1.5

of MIC for complexes and drugs, complexes **1, 3, 4** and **5** gave good results for all microorganisms, among which complex **5** fall out with highest potency against *E. coli*. Reason behind increase in potency of drug is its coordination with metal ion. From the viscosity data of complexes and classical intercalator ethidium bromide; it is clear that all complex show classical intercalative mode of binding, where complex **5** binds more strongly than others complexes. The electronic absorption data are in good accordance with viscosity study. The DNA cleavage study of pUC19 shows that all complexes have high cleavage ability than metal salt and drug. Upon determination of antioxidant activity in NBT/NADH/PMS system, complex **5** shows the highest scavenging ability for oxygen radical. Our group is currently examining a range of biological interactions that these metallointercalators may undergo inside the cell to understand their biochemistry and mechanism of action in better way.

4. Experimental

4.1. Materials and reagents

All solvents, chemicals and reagents used were of analytical reagent grade and were used as such; double distilled water was used throughout. 2,2′-Bipyridylamine (A^6) was purchased from Lancaster (Morecambe, England). Gatifloxacin (GFLH) was generously supplied on demand by Bayer AG (Wuppertal, Germany). Cupric chloride dihydrate was purchased from E. Merck (India) Ltd Mumbai. Pyridine-2-carboxaldehyde (A^8), thiophene-2-carboxaldehyde (A^7), 1,10-phenanthroline, ethidium bromide, bromophenol blue, agarose and Luria Broth were purchased from Himedia, India. 2,9-Dimethyl-4,7-diphenyl-1,10-phenanthroline (A^1) and 2,9-dimethyl-1,10-phenanthroline (A^2), nicotinamide adenine dinucleotide reduced (NADH), nitro blue tetrazolium (NBT) and phenazin methosulfate (PMS) were purchased from Loba chemie PVT. LTD.

4.2. Instrumental measurement

Infrared spectra were recorded on a FT-IR Shimadzu spectrophotometer as KBr pellets in the range 4000–400 cm^{-1}. Elemental analyses (C, H and N) were performed with a model 240 Perkin Elmer elemental analyzer. Metallic content of the complex was determined after decomposing it under effect of acid mixture on heating and titrating against EDTA solution volumetrically and spectrophotometrically using UV-160A UV–vis. spectrophotometer, Shimadzu (Japan) equipped with quartz cells of 1 cm path length. MIC study was carried out by means of laminar air flow cabinet, Toshiba, Delhi, India, Thermogravimetric analyses data were obtained with a model 5000/2960 SDTA, TA instrument (USA). ^1H NMR and ^{13}C NMR were recorded on a Bruker Avance (400 MHz). The electronic spectra were recorded on a UV-160A UV–vis. spectrophotometer, Shimadzu (Japan). Room temperature magnetic measurement for the complexes was made using Gouy magnetic balance. The Guoy tube was calibrated using mercury(II)tetrathiocyanatocobaltate(II) as the calibrant ($\chi_g = 16.44 \times 10^{-6}$ cgs units at 20 °C).[55] FAB-mass spectra were recorded on Jeol SX 102/Da-600 mass spectrophotometer/Data system using Argon/Xenon (6 kV, 10 mA) as the FAB gas. The accelerating voltage was 10 kV and spectra were recorded at room temperature. Photo quantization of the gel after electrophoresis was done using AlphaDigiDoc™ RT. Version V.4.1.0 PC-Image software.

4.3. Ligand preparation

4,5-Diazafluoren-9-one (A^3), 1,10-phenanthroline-5,6-dione (A^4) and 5-nitro-1,10-phenanthroline (A^5) were prepared using reported methods.[56–58]

4.4. Complex preparation

$[Cu(GFL)(A^n)Cl]\cdot 5H_2O$: A methanolic solution of $CuCl_2\cdot 2H_2O$ (1.5 mmol) was added to methanolic solution of neutral bidentate ligand (A^n) (1.5 mmol), followed by addition of a previously prepared solution of gatifloxacin (GFLH) (1.5 mmol) in methanol in presence of CH_3ONa (1.5 mmol). The pH was adjusted to 6.2 using dilute solution of CH_3ONa. The resulting solution was refluxed for 1 h on a steam bath, followed by concentrating it to half of its volume. A fine amorphous product of green color obtained was washed with ether/hexane and dried in vacuum desiccators.

4.5. Spectrophotometric titration

Sample solutions were prepared by decomposing organic matter of complex with acid mixture and making it to total volume of 20 mL with double distilled water. Ten different sets of solutions were prepared by taking a fixed amount of complex solution (2 mL), 2 mL acetate buffer solution and varying aliquots of 0.0005 M EDTA and making it to total volume of 10 mL with double distilled water. Absorbance was measured at 745 nm using buffer as a reference. Amount of copper was determine using the plot of absorbance against volume of EDTA.

4.6. In vitro antimicrobial screening

In the present study, serial tube dilution technique was employed.[59] These tests were performed in triplicate and activities of the compounds were tested against *E. coli*, *P. aeruginosa*, *S. aureus*, *B. Subtilis* and *S. marcescens*. The former three are gram-negative while later two are gram–positive organism. Selection of *E. coli*, *P. aeruginosa* and *S. aureus* are of choice in preliminary screening test organism for several reasons. They are systemic pathogens and seem to develop antibiotic resistance more readily than any other bacteria and laboratory animals can be readily infected with it. The inhibition of growth of this organism produced by various concentrations of the test compounds was compared under identical conditions with inhibition of growth of the same organism in presence of several fluoroquinolone drugs, metal salt, and ligands.

A standard volume (10 mL) of Luria Broth that would support the growth of the test organism was added to several labeled sterile stopper identical assay tubes. Solution of each test compounds was prepared and a series of dilution were prepared. Dilution for metal salts, ligand and standard drugs were also prepared and a control tube containing no test compound was also included. All these operations were carefully performed under aseptic conditions. Assay tubes were incubated at 37 ± 1 °C for 24 h. The resultant faint turbidity was measured. The minimum inhibitory concentration of a test compound is the lowest concentration showing no visible turbidity.

4.7. DNA interaction study

To evaluate the DNA-interaction properties of the synthesized analogues, UV–vis. absorbance titration experiment, viscosity titration and gel electrophoresis; photo quantization techniques were used with pUC19 DNA and were compared within.

4.7.1. Absorbance titration experiment

Binding of DNA via intercalation mode usually results in hypochromism and bathchromism,[60–63] due to the intercalation mode involving a strong stacking interaction between an aromatic chromophore and the DNA base pair.[64] With a selection of an appropriate absorbance peak by performing spectrophotometric wavelength scans of each chelating agents and their Cu(II) complexes. After addition of equivalent amount of DNA to reference cell, kept for 10 min incubation at room temperature followed by absorption measurement. This was specifically done to enable direct comparison between the assays that was required to interpret the results obtained. The intrinsic binding constant, K_b was determine making it subject in following equation.[48]

$$\frac{[DNA]}{(\varepsilon_a - \varepsilon_f)} = \frac{[DNA]}{(\varepsilon_b - \varepsilon_f)} + \frac{1}{K_b(\varepsilon_b - \varepsilon_f)} \quad (1)$$

where [DNA] is the concentration of DNA in terms of nucleotide phosphate [NP], the apparent absorption coefficients ε_a, ε_f, and ε_b correspond to $A_{obs.}/[M]$, the extinction coefficient for free copper complex and the extinction coefficient for free copper complex in fully bound form, respectively and K_b is the ratio of slope to the y intercept.

4.7.2. Viscosity titration

Viscosity measurement is regarded as a reliable tool to determine binding mode in solution state in the absence of crystallographic structural data and NMR data.[65] Viscometric titrations were performed using Ubbelohde viscometer immersed in a thermostatic bath maintained at 27 (±0.1) °C. Flow times were measured with a digital stopwatch, each sample was measured three times, and an average flow time was calculated. Data are presented as $(\eta/\eta_0)^{1/3}$ versus [complex]/[DNA], where η is the viscosity of DNA in the presence of complex and η_0 is the viscosity of DNA alone. Viscosity values were calculated from the observed flowing time of DNA-containing solutions (t) corrected for that of the buffer alone (t_0), $\eta = (t - t_0)$.[65,66]

4.7.3. Gel electrophoresis; photo quantization techniques

Plasmid DNA (pUC19) cleavage activity of $[Cu(GFL)(A^n)Cl]\cdot 5H_2O$ was monitored by agarose gel electrophoresis. In a typical experiment, total volume of 15 μL contain 300 μg/mL of super coiled pUC19 DNA in TE buffer (10 mM Tris, 1 mM EDTA, pH 8.0) treated with different complex (200 μM). The samples were then incubated at 37 °C for 24 h. and loaded on a 1% agarose gel containing 0.5 μg/mL ethidium bromide after quenching the reaction by addition of 5 μL loading buffer (40% sucrose, 0.2% bromophenol blue). Electrophoresis was carried out at 50 V in 1X TAE buffer (0.04 M Tris–Acetate, pH 8, 0.001 M EDTA). Bands were visualized by UV light and photographed followed by the estimation of the intensity of the DNA bands using AlphaDigiDocTM RT. Version V.4.1.0 PC-Image software; gel documentation system.

4.8. SOD-like activity: decomposition of reactive oxygen specie

Superoxide anion ($O_2^{\cdot-}$) was generated in nonenzymatic (PMS/NADH) systems in the presence or absence of test compounds, and scavenging of $O_2^{\cdot-}$ was determined by monitoring reduction in rate of NBT to monoformazan dye formation at 560 nm. The nonenzymatic system contain 30 μM PMS, 79 μM NADH, and 75 μM NBT, phosphate buffer (pH 7.8), and 0.25–5.0 μM tested compound.[48] The reactions were monitored at 560 nm with a UV-160A UV–vis. spectrophotometer, Shimadzu (Japan), and the rate of absorption change was determined. The % inhibition of NBT reduction was calculated using following equation:[67]

$$\%\ \text{Inhibition of NBT reduction} = (1 - k'/k) \times 100\%$$

where k' and k present the slopes of the straight line of absorbance values as a function of time in the presence and absence of SOD mimic compound, respectively. The IC_{50} of the complex was determined by plotting the graph of percentage of inhibiting NBT reduction against the increase in the concentration of the complex. The concentration of the complex which causes 50% inhibition of NBT reduction is reported as IC_{50}.

Acknowledgements

Authors thank Head, Department of Chemistry, and Dr. Thakkar, BRD school of Bioscience, Sardar Patel University, India for making it convenient to work in laboratory and U.G.C. for providing financial support under 'UGC Research Fellowship in Science for Meritorious Students' scheme.

Supplementary data

Supplementary data associated with this article can be found, in the online version, at doi:10.1016/j.bmc.2009.12.037.

References and notes

1. Wolfson, J. S.; Hooper, D. C. *Clin. Microbiol. Rev.* **1989**, *2*, 378.
2. Perry, C. M.; Barman, J. A. B.; Lamb, H. M. *Drugs* **1999**, *58*, 683.
3. *The Merck Index*; Budavari, S., Ed., 13th ed.; Merck and Co.: Whitehouse Station, NJ, 2001.
4. Guo, Z.; Sadler, P. *Angew. Chem., Int. Ed.* **1999**, *38*, 1512.
5. Lippert, B. *Coord. Chem. Rev.* **2000**, *487*, 200.
6. Gellert, M.; Mizuuchi, K.; O'Dea, M. H.; Nash, H. A. *Proc. Natl. Acad. Sci. U.S.A.* **1976**, *73*, 3872.
7. Gellert, M.; Mizuuchi, K.; O'Dea, M. H.; Itoh, T.; Tomizawa, J. *Proc. Natl. Acad. Sci. U.S.A.* **1977**, *74*, 4772.
8. Gillert, M. *Ann. Rev. Biochem.* **1981**, *50*, 879.
9. Cozarelli, N. R. *Science* **1980**, *207*, 953.
10. Palu, G.; Valisena, S.; Ciarrocchi, G. *Proc. Natl. Acad. Sci. U.S.A.* **1992**, *89*, 9671.
11. May, P. M.; Williams, D. R. *Met. Ions Biol. Syst.* **1981**, *12*, 283.
12. Sorenson, J. R. J. *J. Med. Chem.* **1976**, *19*, 135.
13. Brown, D. H.; Lewis, A. E.; Smith, W. E.; Teape, J. W. *J. Med. Chem.* **1989**, *23*, 729.
14. Williams, D. R. *The Metals of Life*, Van Nostrand-Reinhold: London, 1971.
15. Ruiz, M.; Perello, L.; Ortiz, R.; Castineiras, A.; Maichlemossmer, C.; Canton, E. *J. Inorg. Biochem.* **1995**, *59*, 801.
16. Psomas, G.; Raptopoulou, C. P.; Iordanidis, L.; Dendrinou-Samara, C.; Tangoulis, V.; Kessissoglou, D. P. *Inorg. Chem.* **2000**, *39*, 3042.
17. Dendrinou-Samara, C.; Psomas, G.; Raptopoulou, C. P.; Kessissoglou, D. P. *J. Inorg. Biochem.* **2001**, *83*, 7.
18. Schaeffer, P.; Mollet, J.; Aubert, J. P. *Proc. Natl. Acad. Sci. U.S.A.* **1965**, *54*, 704.
19. Sigman, D. S.; Mazumder, A.; Perrin, D. M. *Chem. Rev.* **1993**, *93*, 2295.
20. (a) Fridovich, I. *Annu. Rev. Biochem.* **1995**, *64*, 97; (b) Miller, A. F. *Comments Mol. Cell. Biophys.* **1997**, *9*, 1; (c) Valentine, J. S.; Wertz, D. L.; Lyons, T. J.; Liou, L.; Goto, J. J.; Gralla, E. B. *Curr. Opin. Chem. Biol.* **1998**, *2*, 253; (d) Miller, A. F. *Curr. Opin. Chem. Biol.* **2004**, *8*, 162.
21. (a) McCord, J. M. *Methods Enzymol.* **2002**, *349*, 331; (b) Bayer, W.; Imlay, J.; Fridovich, I. *Prog. Nucleic Acid Res. Mol. Biol.* **1991**, *40*, 221; (c) Wallace, D. C. *Science* **1992**, *256*, 628; (d) Winterbourn, C. C. *Free Radical Biol. Med.* **1993**, *14*, 85; (e)*Active Oxygen in Biochemistry*; Halliwell, B., Valentine, J. S., Foote, C. S., Greenberg, A., Liebman, J. F., Eds.; Blackie Academic and Professional: New York, 1995; pp 336–400.
22. Abuhijleh, A. L. *J. Inorg. Biochem.* **1997**, *68*, 167.
23. Bhirud, R. G.; Srivastava, T. S. *Inorg. Chim. Acta* **1991**, *179*, 125.
24. Patel, R. N.; Singh, N.; Shukla, K. K.; Chauhan, U. K.; Niclós-Gutiérrez, J.; Castiñeiras, A. *Inorg. Chim. Acta* **2004**, *357*, 2459.
25. Casanova, J. C.; Alzuci, G.; Borrás, J.; Latorre, J.; Sanau, M.; Garcıa-Granda, S. *J. Inorg. Biochem.* **1995**, *60*, 219.
26. Mendhum, J.; Denney, R. C.; Barnes, J. D.; Thomas, M. J. K. *Vogel's Text Book Of Quantitative Chemical Analysis*, 6th ed.; Pearson Education PVT LTD: Singapore, India, 2002; pp 312–460.

27. Day, R. A., Jr.; Underwood, A. L. *Quntitative Analysis*, 6th ed.; Prentice-Hall of India PVT LTD, 2006; pp 388–441.
28. Nakamoto, K. *Infrared and Raman spectra of inorganic and coordination compounds*, 4th ed.; A Wiley Interscience Publication: New York, 1986.
29. Patel, S. H.; Pansuriya, P. B.; Chhasatia, M. R.; Parekh, H. M.; Patel, M. N. *J. Therm. Anal. Calorim.* **2008**, *91*, 413.
30. Turel, I.; Leban, I.; Bukovec, N. *J. Inorg. Biochem.* **1997**, *66*, 241.
31. Freedman, H. H. *J. Am. Chem. Soc.* **1961**, *83*, 2900.
32. Chandra, S.; Gupta, N.; Gupta, L. K. *Synth. React. Inorg. Met.-Org. Chem.* **2004**, *34*, 919.
33. Iskander, M. F.; EL-Sayed, L.; Salem, N. M. H.; Warner, R. W. *J. Coord. Chem.* **2005**, *58*, 125.
34. Mendoza-Diaz, G.; Martineza-Auguilera, L. M. R.; Perez-Alonso, R.; Solans, X.; Moreno-Esparza, R. *Inorg. Chim. Acta* **1987**, *138*, 41.
35. Melnik, M. *Coord. Chem. Rev.* **1981**, *36*, 1.
36. Carballo, R.; Castineiras, A.; Covelo, B.; Garcia-Martinez, E.; Niclos, J.; Vazquez-Lopez, E. M. *Polyhedron* **2004**, *23*, 1505.
37. Figgis, B. N.; Lewis, J. In *Modern Coordination Chemistry: Principles and Methods*; Lewis, J., Wilkins, R. G., Eds.; Interscience: New York, 1960.
38. Psomas, G.; Dendrinou-Samara, C.; Philippakopoulos, P.; Tangoulis, V.; Raptopoulou, C. P.; Samaras, El.; Kessissoglou, D. P. *Inorg. Chim. Acta* **1998**, *272*, 24.
39. Russell, A. D. In *Disinfection, Sterilization and Preservation*; Block, S. S., Ed., 4th ed.; Lea and Febinger: Philadelphia, 1991; pp 27–59.
40. Rossmore, H. W. In *Disinfection Sterilization and Preservation*; Block, S. S., Ed., 4th ed.; Lea and Febinger: Philadelphia, 1991; pp 290–321.
41. *Circular Dichroism and Linear Dichroism*; Rodger, A., Norden, B., Eds.; Oxford University Press: Oxford, 1997.
42. Song, G.; He, Y.; Cai, Z. *J. Fluoresc.* **2004**, *14*, 705.
43. Jenkins, T. C. In *Drug–DNA Interaction Protocols*; Fox, K. R., Ed.; Humana Press: Totowa, NJ, 1997; pp 195–218.
44. Son, G. S.; Yeo, J. A.; Kim, M. S.; Kim, S. K.; Holmen, A.; Akerman, B.; Norden, B. *J. Am. Chem. Soc.* **1998**, *120*, 6451.
45. El-Metwaly, N. M. *Trans. Met. Chem.* **2007**, *32*, 88.
46. Patra, A. K.; Dhar, S.; Nethaji, M.; Chakravarty, A. R. *Dalton Trans.* **2005**, 896.
47. Hirohama, T.; Karunuki, Y.; Ebina, E.; Suzaki, T.; Arii, H.; Chikira, M.; Selvi, P. T.; Palaniandavar, M. *J. Inorg. Biochem.* **2005**, *99*, 1205.
48. Ihmels, H.; Otto, D. *Top. Curr. Chem.* **2005**, *258*, 161.
49. Palchaudhuri, R.; Hergenrother, P. J. *Curr. Opin. Biotechnol.* **2007**, *18*, 497.
50. Wheate, N. J.; Brodie, C. R.; Collins, J. G.; Kemp, S.; Aldrich-Wright, J. R. *Mini-Rev. Med. Chem.* **2007**, *7*, 627.
51. Basili, S.; Bergen, A.; Dall'Acqua, F.; Faccio, A.; Ranzhan, A.; Ihmels, H.; Moro, S.; Viola, G. *Biochemistry* **2007**, *46*, 12721.
52. Hertzberg, R. P.; Dervan, P. B. *J. Am. Chem. Soc.* **1982**, *104*, 313.
53. Sigman, D. S.; Graham, D. R.; Marshall, L. E.; Reich, K. A. *J. Am. Chem. Soc.* **1980**, *102*(16), 5419.
54. Figgis, B. N.; Nyholm, R. S. *J. Chem. Soc.* **1958**, 4190.
55. Henderson, L. J., Jr.; Fronczek, F. R.; Cherry, W. R. *J. Am. Chem. Soc.* **1984**, *106*, 5876.
56. Hiort, C.; Lincoln, P.; Norden, B. *J. Am. Chem. Soc.* **1993**, *115*, 3448.
57. Smith, G. F.; Cagle, F. W. M. J. R. J. *Org. Chem.* **1947**, *12*(6), 781.
58. Pelczar, M. J.; Reid, R. D.; Chan, E. C. S. *Microbiology*, 4th ed.; Tata McGraw-Hill: New Delhi, 1979.
59. Trommel, J. S.; Marzilli, L. G. *Inorg. Chem.* **2001**, *40*, 4374.
60. Mudasir; Yoshioka, N.; Inoue, H. *J. Inorg. Biochem.* **1999**, *77*, 239.
61. Jin, L.; Yang, P. *J. Inorg. Biochem.* **1997**, *68*, 79.
62. Zhang, Q. L.; Liu, J. G.; Chao, H.; Xue, G. Q.; Ji, L. N. *J. Inorg. Biochem.* **2001**, *83*, 49.
63. Shi, S.; Liu, J.; Li, J.; Zheng, K.; Huang, X.; Tan, C.; Chen, L.; Ji, L. *J. Inorg. Biochem.* **2006**, *100*, 385.
64. Wolfe, A.; Shimer, G. H., Jr.; Meehan, T. *Biochemistry* **1987**, *26*, 6392.
65. Basili, S.; Bergen, A.; Dall'Acqua, F.; Faccio, A.; Ranzhan, A.; Ihmels, H.; Moro, S.; Viola, G. *Biochemistry* **2007**, *46*, 12721.
66. Huguet, A. I.; Manez, S.; Alcaraz, M. J. *Z. Naturforsch.* **1990**, *45*, 19.
67. Le, X.; Liao, S.; Liu, X.; Feng, X. *J. Coord. Chem.* **2006**, *59*(9), 985.